Redox Biology 77 (2024) 103363

Contents lists available at ScienceDirect

Redox Biology

journal homepage: www.elsevier.com/locate/redox

Lycopene alleviates age-related cognitive deficit via activating liver-brain fibroblast growth factor-21 signalling

Jia Wang [a,b,*], Lu Li [a], Li Li [a], Yuqi Shen [a], Fubin Qiu [a,b,**]

[a] Nutritional and Food Sciences Research Institute, Department of Nutrition and Food Hygiene, School of Public Health, Shanxi Medical University, Taiyuan, 030001, China

[b] MOE Key Laboratory of Coal Environmental Pathogenicity and Prevention, School of Public Health, Shanxi Medical University, Taiyuan, 030001, China

ARTICLE INFO

Keywords:
Synaptic vesicle fusion
Neurotransmitters
Liver-brain FGF21 signalling
Lycopene
Aging

ABSTRACT

Brain function is linked with many peripheral tissues, including the liver, where hepatic fibroblast growth factor 21 (FGF21) mediates communication between the liver and brain. Lycopene (LYC), a naturally occurring carotenoid, posses multiple health-promoting properties, including neuroprotective function. Here, we investigated the effects of LYC on age-related memory impairment and the relative contribution of liver-brain FGF21 signaling in these process. The results showed that after treatment with LYC for 3 months, brain aging and age-related cognitive deficits were effectively managed. In addition, LYC ameliorated neuronal degeneration, mitochondrial dysfunction and synaptic damage, and promoted synaptic vesicle fusion in 18-month-old mice. Notably, LYC activated liver-brain FGF21 signalling in aging mice. Whereas all these central effects of LYC were negated by blocking FGF21 via *i. v.* injection of adeno-associated virus in aging mice. Furthermore, recombinant FGF21 elevated mitochondrial ATP levels and enhanced synaptic vesicle fusion in mouse hippocampal HT-22 cells, which promoted neurotransmitter release. Additionally, we co-cultured hepatocytes and neurons in Transwell and found that LYC enhanced hepatocytes' support for neurons. This support included improved cell senescence, enhanced mitochondrial function, and increased axon length in co-cultured neurons. In conclusion, LYC protects against age-related cognitive deficit, partly explained by activating liver-brain FGF21 signalling, hence promoting neurotransmitters release via increasing mitochondrial ATP levels and enhancing synaptic vesicle fusion. These findings revealed that FGF21 could be a potential therapeutical target in nutritional intervention strategies to improve cognitive damage caused by aging and age-related neurodegenerative diseases.

1. Introduction

Aging is irreversible and natural, accompanied by a gradual decline in various tissues [1]. The ageing of the global population increases the risk of age-related diseases, posing significant health challenges [2]. In addition, sex differences influence the development of aging-induced dementia, with women likely to have more severe cognitive impairment [3]. Therefore, understanding the pathological mechanism in aging females and developing interventions to delay it is important in this field [3]. Notably, nutritional interventions including phytochemical supplements, are widely used to delay aging and age-related diseases [4]. Lycopene (LYC), a carotenoid, is abundant in many fruits and vegetables [5]. It can effectively scavenge free radicals as a result of its unique chemical structure [5,6], and other multiple health benefits, such as alleviating inflammatory responses [5,6], glycolipid metabolism regulation [7], and neuroprotective effects [8–10]. These benefits have made it the focus of public health research. Notably, studies show that LYC effectively combats aging and age-related disorders [11,12]. Findings from our recent research revealed that LYC (0.03 %) supplementation for 8 weeks reduced cognitive deficit in D-galactose-induced aging in mice [10].

Brain function is linked with many peripheral tissues, including the

* Corresponding author. Nutritional and Food Sciences Research Institute, Department of Nutrition and Food Hygiene, School of Public Health, Shanxi Medical University, Taiyuan, 030001, China.

** Corresponding author. Nutritional and Food Sciences Research Institute, Department of Nutrition and Food Hygiene, School of Public Health, Shanxi Medical University, Taiyuan, 030001, China.

E-mail addresses: WangjiaSXMU@aliyun.com (J. Wang), 18392650556@163.com (F. Qiu).

https://doi.org/10.1016/j.redox.2024.103363
Received 21 August 2024; Received in revised form 17 September 2024; Accepted 18 September 2024
Available online 19 September 2024

liver [13,14], through metabolic, hormonal, immunological and inflammatory pathways [14]. Furthermore, recent clinical and basic research findings showed that liver disease phenotypes and neurodegenerative disease were strongly correlated. However, the mediators and critical pathways involved are not well understood [15]. Fibroblast growth factor-21 (FGF21), a metabolic regulator, is produced in the liver, adipose tissue, pancreas, and heart muscle [16,17]. Notably, it is present in human and rodent cerebrospinal fluid (CSF) [18]. Furthermore, a linear relationship exists between serum FGF21 levels and CSF FGF21 levels in humans [16]. Moreover, Liang et al. reported that fasting greatly increased FGF21's hypothalamic level, and FGF21 mRNA expression was not detected in this tissue even in the fasted state [18]. This revealed that FGF21 in the brain is transferred from peripheral tissue. In addition, FGF21 is synthesized in multiple organs, under normal physiologic conditions, however, circulating FGF21 comes from the liver [19,20]. It crosses the blood-brain barrier (BBB) by simple diffusion [21] and reaches the brain directly, exerting its effects on central nervous system (CNS) [22,23]. Thus, the hepatic FGF21 is signal effectively links the liver with CNS [16,18,24]. Furthermore, FGF21, a pro-longevity hormone, improves neurological diseases-associated

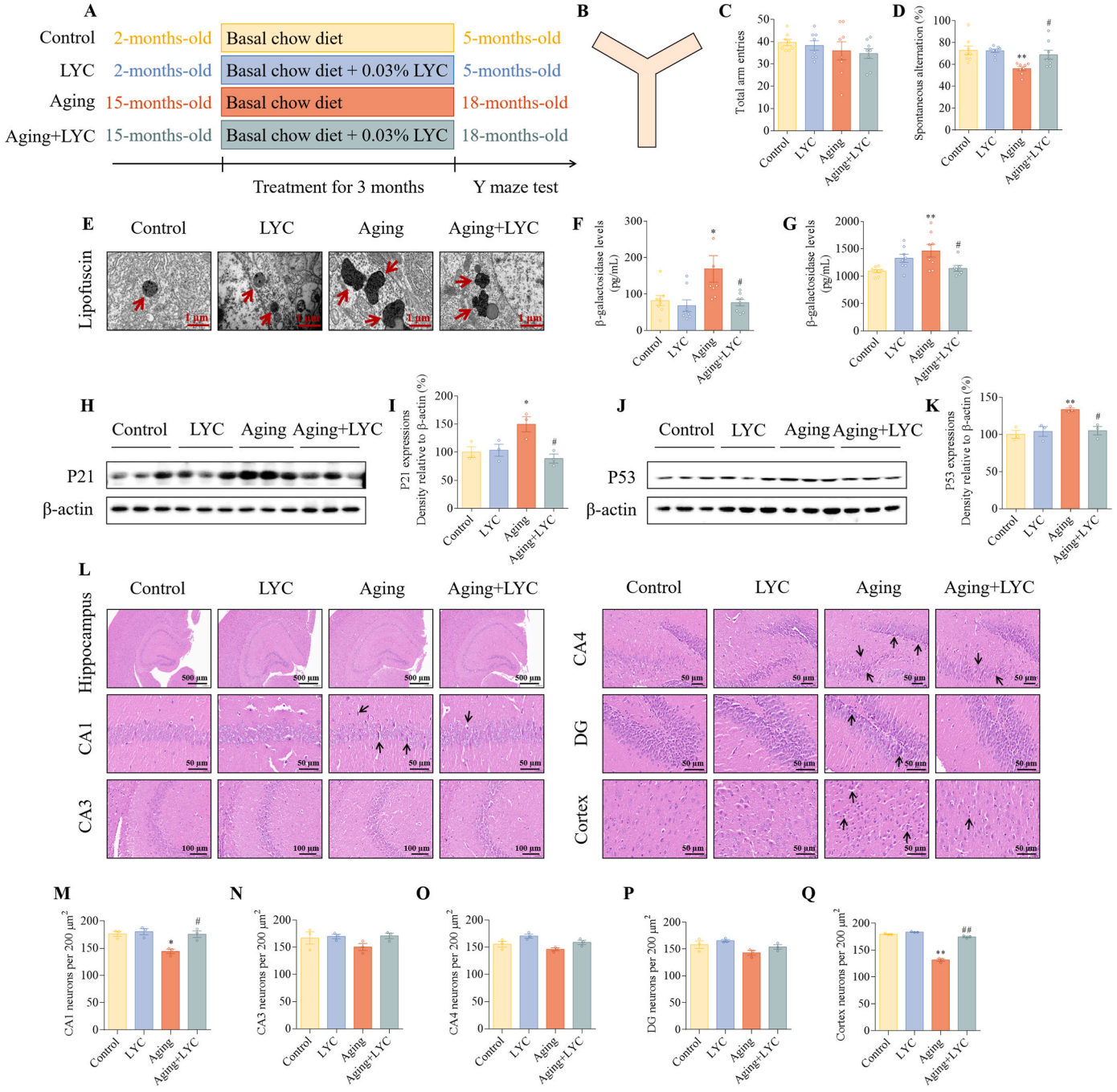

Fig. 1. Effects of LYC on the spatial memory impairment of aging mice.
(A) Experimental scheme. (B) Schematic diagram of the Y maze. (C) Total arm entries and (D) spontaneous alternation in Y maze. (E) Representative electron micrograph of lipofuscin in hippocampus (the arrows indicated lipofuscin), n = 6. SA-β-gal levels in the (F) cortex of mice and (G) plasma. Proteins expressions of (H) P21 and (J) P53 in cortex. Densitometry analyses were shown in (I) and (K). (L) H&E staining analysis of neurons in hippocampus and cortex (the arrows indicated shrunken and deformed neuronal cells), n = 3. (M–Q) Neurons in hippocampus and cortex. $^{*}p < 0.05$, $^{**}p < 0.01$ versus Control group, $^{\#}p < 0.05$, $^{\#\#}p < 0.01$ versus Aging group.

synaptic plasticity [25,26]. Hence, it has been studied as a potential therapeutic molecule for aging and CNS disorders. However, numerous studies focus on the direct effects on brain function through pharmacological administration. The FGF21-induced liver-brain interaction remain unexplored.

Hence, in this study, we aimed to evaluate the protective effects of LYC supplementation on aging-associated cognitive decline and investigate whether hepatic FGF2 critically mediates brain function by (a) examining the effects of LYC on memory deficits, brain aging, neuronal degeneration, synaptic structural integrity, synaptic vesicle fusion and liver-brain FGF21 signalling in aging mice; (b) knockdown of FGF21 using tail vein injection of adeno-associated virus (AAV) to determine whether hepatic FGF21 mediates LYC's brain benefits, revealing the target of hepatic FGF21; (c) recombinant FGF21 incubated with mouse hippocampal HT-22 cells to uncover its effects on synaptic vesicle fusion and neurotransmitters release; and (d) investigating the functional support of hepatocytes to neuronal cells through performing hepatocyte-neurons co-culture experiments in Transwell. The present study provided novel insights into the mechanism of LYC on the intervention of aging-related cognition decline and synaptic damage.

2. Materials and methods

2.1. Short hairpin design and adeno-associated virus production

The FGF21 sequence (*Mus musculus*, NCBI Gene ID: 56636) was analyzed to identify possible sequences for RNA interference-mediated silencing. A negative control (NC, 5′-TTCTCCGAACGTGTCACGT-3′) or shFGF21 (5′-GGGATTCAACACAGGAGAAAC-3′) with a TTCAAGAGA hairpin loop and TTTTTT termination sequence were generated, annealed, and cloned into a pAAV-U6-eGFP entry vector (Shanghai GenePharma Co., Ltd). All viruses were purified using a discontinuous CsCl gradient after plaque selection and amplification [26].

2.2. Animal model and experimental design

For the first set of animals, female CD-1 mice were acquired from the Beijing Vital River Laboratory Animal Technology (Beijing, China). These animals were allowed to acclimatize for 1 week under standard conditions (12 h light/dark cycle, temperature 22 ± 2 °C and humidity 40 %–50 %). Subsequently, they were divided into four groups (10 mice/group): a young Control group (2-month-old) and Aging group (15-month-old) fed with a commercial normal chow diet. Furthermore, mice in the LYC group (2-month-old) and Aging + LYC group (15-month-old) were fed with 0.03 % LYC (w/w, mixed with normal chow diet) for 3 months (Fig. 1A). The purity of LYC was >95 % and was obtained from Yuanye Biological Technology Co., Ltd. (Shanghai, China).

The second set of mice (15-month-old) were treated with AAV-shFGF21 (5×10^9 plaque-forming units viruses per mouse, tail vein injection) [26] and received the same regimen of LYC intervention (10 mice/group). The AAV injections were administered twice, one before adaptive feeding and one mid-way through the experiment (Fig. 6A) [26].

All experiments were performed following the Guide for the Care and Use of Laboratory Animals (8th edition, ISBN-10: 0-309-15396-4). The study proposal was done following the Regulations on the Administration of Laboratory Animals and approved by the Research Involving Animals of Shanxi Cancer Hospital (IACUC-2022003).

2.3. Cell culture

LYC was dissolved in dimethylsulfoxide. Cells were cultured in DMEM medium with 10 % foetal bovine serum, 1 % penicillin and streptomycin at 37 °C. Furthermore, the cells were supplemented with 5 % CO_2. HT-22 cells were incubated with 100 nM recombinant human FGF21 (rFGF21) [26] and D-galactose (D-gal) for 8 h. In HepG2-HT-22 co-culture experiments, HepG2 cells were incubated with LYC and D-gal for 8 h.

2.4. Behavioral experiments

The Y-maze apparatus, which comprised three arms, was used for this experiment (Fig. 1B). Each mouse was allowed to explore the Y-maze for 10 min freely during the test phase for assessment of spatial working memory. Subsequently, the percentage of alternation and total number of arm entries were analyzed.

2.5. Western blotting analysis

Proteins were separated by sodium dodecyl sulfate (SDS)-polyacrylamide gel electrophoresis and transferred onto a polyvinylidene fluoride membrane. These membranes were incubated with appropriate and secondary antibodies. Furthermore, positive bands were visualized with an enhanced chemiluminescence reagent. Detailed antibodies information used in this study can be obtained from the **Supplementary information**.

2.6. Electron microscopy of hippocampal ultrastructure

The hippocampus of each mouse was cut into 1 mm^3 pieces and fixed in a fixative solution at 4 °C. Subsequently, the tissue was placed in 1 % osmium tetraoxide and were embedded within epoxy resin. Ultrathin sections were made and stained with both uranyl acetate and lead citrate. The ultrastructure of hippocampus was observed by using a transmission electron microscope.

2.7. Haematoxylin and eosin staining and Nissl staining

The fixed tissues were processed, embedded in paraffin and cut into 5 μm sections. The sections were stained with haematoxylin for haematoxylin and eosin (H&E) staining and were stained with Nissl staining solution for Nissl staining analysis.

2.8. Immunohistochemical staining and immunofluorescence staining

Fixed tissue sections or cells were stained with appropriate primary antibodies at 4 °C overnight. For immunohistochemical staining, tissue sections were exposed to secondary antibodies, visualized using chromogen 3,3′-diaminobenzidine (DAB) (DAB kit, Zhongshan Golden Bridge biotechnology Co. Ltd., Beijing, China), counterstained with haematoxylin solution and observed under a light microscope. For immunofluorescence staining, tissue sections or cells incubated with appropriate secondary antibodies and immunofluorescence images were acquired using an inverted fluorescent microscope. Quantitative immunohistochemical and immunofluorescence analysis were performed by using ImageJ software.

2.9. Co-Immunoprecipitation

Protein lysates were used for Co-Immunoprecipitation (Co-IP) analysis. Primary antibodies were added to the protein A/G Magnetic Beads. Furthermore, suspensions from the lysate were added to the protein A/G Magnetic Beads after rotating at 4 °C for 8 h. Subsequently, the resulting mixture was rotated overnight at 4 °C. Elution of the reactive proteins was performed by re-suspending the beads in protein sample buffer, followed by boiling for 5 min. The supernatant was then resolved on a 10 % SDS-polyacrylamide gel and treated as indicated above for western blotting.

2.10. Cell viability assay

Cell viability was expressed as a percentage of the control group (untreated cells). Cells were seeded into 96-well plate at a density of 1×10^4 cells/well. Additionally, cells were incubated with 10 % CCK-8 labelling reagent (MA0218, meilunbio; China) at 37 °C for 1 h after different concentrations of LYC or D-gal treatment. The absorbance of the mixture at 450 nm was measured using a microplate reader.

2.11. Analyzsis of mitochondrial morphology

Cells were seeded in confocal dishes and subsequently loaded with 100 nM Mito-tracker greens probe (C1048, Beyotime Biotechnology, Shanghai, China) for 30 min and then co-stained with Hoechst. The morphology of mitochondria was further observed under a confocal fluorescence microscope.

2.12. Determination of total and mitochondrial reactive oxygen species content

Cells were incubated with 10 μM DCFH-DA fluorescent probe (S0033S, Beyotime Biotechnology, Shanghai, China) or 5 μM MitoSOX red fluorescent probe (S0061S, Beyotime Biotechnology, Shanghai, China) respectively for 30 min in the dark. This incubation was done to analyze the levels of intracellular total reacting oxygen species (ROS) or mitochondrial ROS, which was observed with a fluorescence microscope. Quantitative analysis of mitochondrial ROS and total ROS were performed by using ImageJ software.

2.13. JC-1 staining and β-galactosidase staining

The JC-1 staining was performed by incubating cells with 10 μg/mL JC-1 staining (C2005, Beyotime Biotechnology, Shanghai, China) for 1.5 h in the dark and observed using a fluorescence microscope. Furthermore, cells were incubated with senescence-associated-beta-galactosidase (SA-β-gal) staining solution for 48 h and observed with a light microscope for β-galactosidase staining. Quantitative analysis of mitochondrial membrane potential in HT-22 cells were performed by using ImageJ software.

2.14. Biochemical indexes assay

Enzyme-linked immunosorbent assay (ELISA) kits for BDNF, NGF, interleukin 1beta (IL-1β), FGF21, β-galactosidase, neurotransmitters, adenosine triphosphate (ATP) synthase, ATP, interleukin 6 (IL-6), and tumor necrosis factor alpha (TNFα) were purchased from Meimian Industrial Company (Jiangsu, China). Kits for glutathione (GSH) (A006-2), total antioxidant capacity (T-AOC) (A015-2-1), malondialdehyde (MDA) (A003-1-2), catalase (CAT) (A007-2) and superoxide dismutase (SOD) (A001-3) were purchased from Jiancheng Bioengineering (Nanjing, China). Biochemical indexes assays in tissues, cells, and medium were performed following the manufacturer's instructions.

2.15. Complex molecular modeling simulation

The flexibility and general stability of the docked complexes were assessed using complex molecular modeling (MD) simulations spanning 100 ns with AutoDock Vina. Simulations described herein were obtained from GROMACS 2021 using CHARM36 m force field. Complexes were solvated with TIP3P water cubic box with dimension boundaries extended to 10 Å from protein atoms and neutralized with counterions, Na^+/Cl^-. Furthermore, the complexes were initially subjected to energy minimization (500 fs) to eliminate irrational atomic connections. An isothermal-isobaric (NPT) ensemble was used to equilibrate the prepared system after a canonical (NVT) ensemble. Lastly, 100 ns MD simulations were performed with a 2-fs time step at normal temperature and pressure (310 K and 1.01325 bar, respectively).

2.16. Statistical analysis

Data from mouse brains were presented as the means ± SEM of at least three independent experiments, and data in cells were presented as the means ± SD. Differences among the three groups were statistically analyzed by one-way analysis of variance followed by Tukey's test using GraphPad Prism 8 software, and statistical significance was set at $p < 0.05$.

3. Results

3.1. Dietary LYC alleviated age-induced spatial memory deficits and improved brain aging

The Y-maze test was used to evaluate the effects of LYC on working memory. Results showed that there were no significant difference about total arm entries among groups (Fig. 1C). Furthermore, aging mice showed impaired spatial cognition with a significantly down-regulated spontaneous alternation ($p < 0.01$) (Fig. 1D) compared with the young control group. However, LYC markedly stimulated the decreased spontaneous alternation ($p < 0.05$) (Fig. 1D) and ameliorated working memory impairment. Lysosomal content including SA-β-gal activities and lipofuscin will increased during aging as a result of the accumulation of old lysosomes [27]. The lipofuscin content in the hippocampus of aging group mice was increased when compared with those of the young control group (Fig. 1E). Consistently, aging mice also showed elevated SA-β-gal levels in the cortex of mice and plasma (Fig. 1F and G). Furthermore, LYC administration reduced the levels of lipofuscin and SA-β-gal. LYC also markedly down-regulated the expressions of age-related proteins P21 (Fig. 1H and I) and P53 (Fig. 1J and K) in the cortex, indicating that LYC has a positive protective effect on brain aging.

3.2. Dietary LYC alleviated neuronal degeneration and synaptic damage

H&E staining was performed to investigate the histopathology changes in the hippocampus and cortex. As demonstrated in Fig. 1L, there were no marked morphological changes in the young control group and LYC group. In contrast, significant neuronal nuclei shrinkage was detected in aging mice (arrows indicate shrunken and deformed neuronal cells). In addition, aging led to reduction in surviving neurons in the cortex and hippocampal regions (Fig. 1M–Q), however, LYC supplementation protected against aging-induced neuronal degeneration and loss. Furthermore, neurotrophic factors are involved in neurogenesis and neuronal plasticity [28]. As presented in Fig. 2, a decreased levels of BDNF in the hippocampus and cortex, decreased levels of NGF in the cortex were observed in aging mice. However, LYC treatment partly rescued the down-regulation of these neurotrophic factors. Furthermore, analysis of hippocampal synaptic ultrastructure (Fig. 3A–C) revealed that LYC increased the length and width of post-synaptic density (PSD) of mice compared with those in aging group (red arrows indicated PSD). The expressions of synapse marker proteins PSD-95 were also elevated in the cortex (Fig. 3D–G) and hippocampus (S. Fig. 1A–D) of Aging + LYC group mice.

3.3. Dietary LYC promoted synaptic vesicle fusion in aging mice

Neuronal communication depends on the precise regulation of synaptic vesicle fusion and neurotransmitters release [29]. As presented in Fig. 3A, accumulated synaptic vesicles were observed at presynaptic sites in the aging group (green arrows indicated synaptic vesicles), indicating that the synaptic vesicle fusion processes were blocked. However, LYC intervention mitigated the accumulation of synaptic vesicles. We analyzed the key proteins involved in neurotransmitters

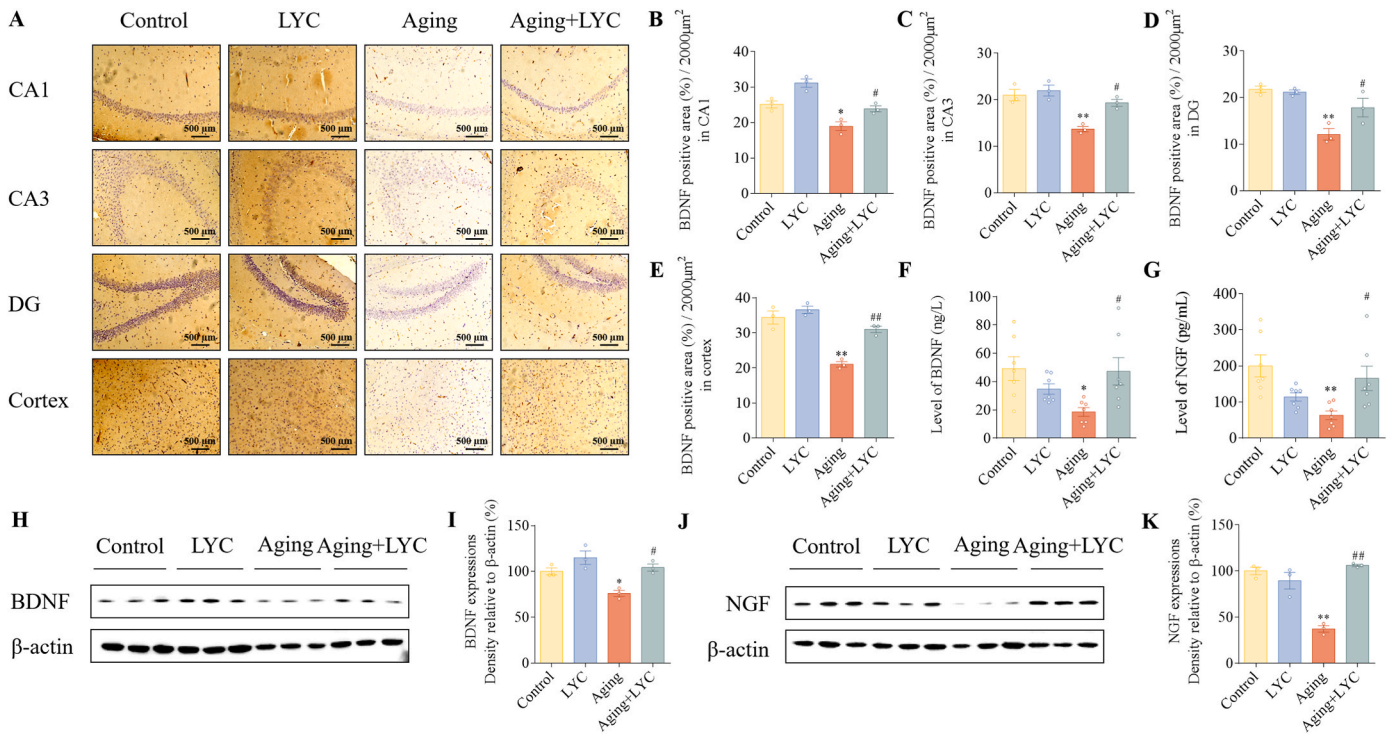

Fig. 2. Effects of LYC treatment on neurotrophic factors
(A) Immunohistochemical staining of BDNF in the hippocampus and cortex of mice. Quantitative immunohistochemical analysis for evaluating BDNF expression in (B) CA1, (C) CA3, (D) DG and (E) cortex regions. ELISA kits assay for (F) BDNF and (G) NGF levels in the cortex. Protein expressions of (H) BDNF and (J) NGF in the cortex. Densitometry analyses were shown in (I) & (K). $^{*}p < 0.05$, $^{**}p < 0.01$ versus Control group, $^{\#}p < 0.05$, $^{\#\#}p < 0.01$ versus Aging group.

release to reveal the mechanisms by which LYC modifies synaptic vesicles, including synaptic soluble N- ethylmaleimide-sensitive factor attachment protein receptors (SNAREs) core complex SNAP-25, synaptobrevin (VAMP), and syntaxin, which are responsible for neurotransmitters release by bringing synaptic vesicles and plasma membranes together and catalyzing membrane fusion [30]. Results showed that LYC substantially elevated aging-decreased protein expressions of SNAP-25 in the cortex (Fig. 3H–K) and hippocampus (S. Fig. 1E–H), increased the protein expression of VAMP in the cortex of mice (Fig. 3L and M), however, no effects on the protein expression of syntaxin in cortex was observed (Fig. 3L and N). Notably, LYC enhanced the associativity of SNAP-25, syntaxin and VAMP (Fig. 3O–R) in the cortex of mice. Further more, Munc18 regulates synaptic vesicle priming via binding to syntaxin and forms a template to assemble SNAREs complex [30,31]. Here, we also explored the effects of LYC on the interaction between Munc18 and syntaxin in hippocampus, results showed that there were no significant differences about the colocalization of green (Munc18) and red (syntaxin) fluorescence signals among groups (Fig. 3S).

3.4. Dietary LYC improved aging-caused mitochondrial dysfunction

In addition to SNAREs complex, substantial mitochondrial ATP consumption is required for synaptic vesicle recycling and neurotransmitter refilling [32]. Thus, mitochondrial dysfunction are also involved in the development and progression of aging-induced cognitive impairment [33]. As illustrated in Fig. 4A–C, the mitochondria in the control group and LYC group had well-defined cristae and well-preserved surrounding membranes. Furthermore, mitochondrial swelling and vacuolation were observed in the aging group. Treatment with LYC improved mitochondrial morphological damage. Additionally, aging decreased the levels of mitochondrial electron transport chain complex (Fig. 4D–G), down-regulated the level of ATP synthase (Fig. 4H) and suppressed the production of ATP (Fig. 4I) in the cortex of mice, besides, LYC treatment significantly reversed these changes, indicating that LYC has protective effect on mitochondrial function.

3.5. LYC relieved neuroinflammation and oxidative stress induced by aging

Neuroinflammation and oxidative stress are associated with the accumulation of damaged neuronal components and cognitive decline [34]. Microglia and astrocytes are key regulators of inflammatory responses in the CNS [35]. Here, LYC treatment effectively suppressed the over-activation of microglia (S. Fig. 2A–D) and astrocytes (S. Fig. 2E–H) in hippocampus, down-regulated the levels of inflammatory factors IL-1β (Fig. 4J–L), COX-2 (Fig. 4K and M), IL-6 (Fig. 4N) and TNFα (Fig. 4O) in the cortex of mice. The Nrf2/HO-1 pathway is implicated in maintaining redox homeostasis and a blocked Nrf2/HO-1 results in enhanced oxidative stress [36]. LYC activated Nrf2/HO-1 signal in the cortex of mice (Fig. 4P–R), up-regulated the activities of antioxidant enzyme SOD and CAT, increased the levels of GSH in the cortex and plasma (Fig. 4S–X). In addition, it also increased the level of T-AOC (Fig. 4Y) and decreased the levels of MDA (S. Fig. 2I) and H_2O_2 (Fig. 4Z) in the cortex of mice.

3.6. LYC activated FGF21 signal in liver-brain-axis

We examined the effects of LYC on liver-brain axis FGF21 signalling and found that LYC elevated FGF21 levels in the cortex of mice (Fig. 5A–E) and plasma (Fig. 5F) compared with those of the Aging group. The histological analyses showed significantly elevated hepatocyte necrosis, microvesicular steatosis, inflammatory cell infiltration and fibrosis in aging mice. However, supplementing of LYC for 3 months could significantly improve these changes (Fig. 5G). Peroxisome proliferator-activated receptor alpha (PPARα), a key mediator of FGF21 in the liver [24], can be modulated by multiple natural products [37,38]. In the present study, LYC elevated the protein expression of hepatic

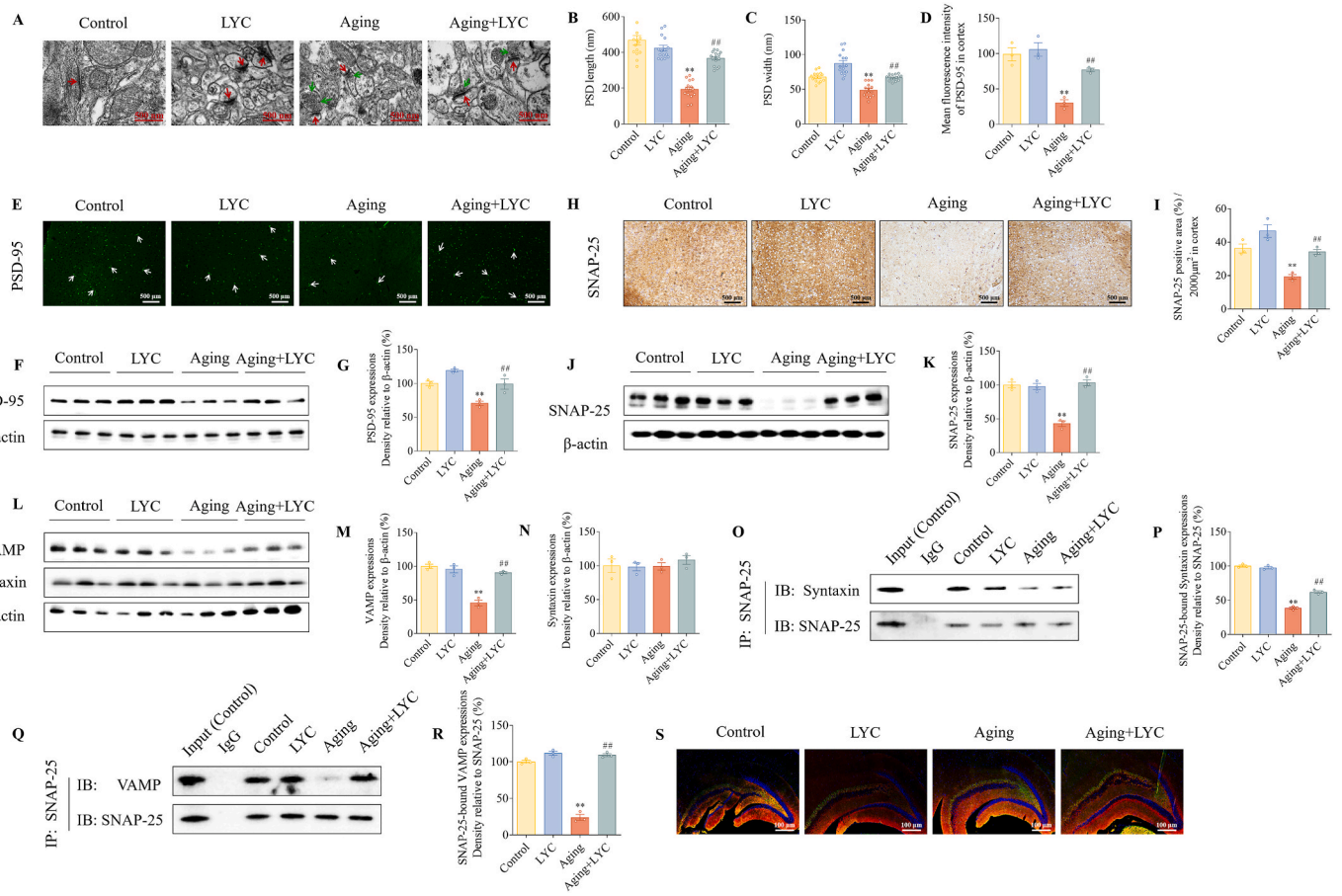

Fig. 3. Effects of LYC on neuronal degeneration and synaptic vesicle fusion.
(A) Representative electron micrograph of synaptosomal fractions from mice hippocampus (the red arrows indicated PSD and green arrows indicated synaptic vesicle), n = 6. (B) The length of PSD. (C) The width of PSD. (D) Quantitative immunofluorescence analysis for evaluating PSD-95 expression in cortex. (E) Immunofluorescence staining of PSD-95 in cortex (the arrows indicated PSD-95 protein), n = 3. (F) Protein expression of PSD-95 in cortex. Densitometry analysis was shown in (G). (H) Immunohistochemical staining of SNAP-25 in cortex, n = 3. (I) Quantitative immunohistochemical analysis for evaluating SNAP-25 expression in cortex. (J) Protein expression of SNAP-25 in cortex. Densitometry analysis was shown in (K). (L) Protein expressions of VAMP and syntaxin in cortex. Densitometry analyses were shown in (M)&(N). Co-IP and western blots analysis were used to evaluate the associativity of SNAP-25 and syntaxin (O)&(P), SNAP-25 and VAMP (Q)&(R) in cortex. (S) Immunofluorescence co-localization analysis for syntaxin (red fluorescence signals) and Munc18 (green fluorescence signals) in hippocampus, n = 3. $^{*}p < 0.05$, $^{**}p < 0.01$ versus Control group, $^{\#}p < 0.05$, $^{\#\#}p < 0.01$ versus Aging group.

PPARα (Fig. 5H, I, K, L). LYC also up-regulated the mRNA (Fig. 5N) and protein (Fig. 5H–J, K, M) expressions of hepatic FGF21.

To get a more realistic picture of the interactions between PPARα protein and LYC, the docked complexes were simulated in a water box for about 100 ns. The root mean square deviation (RMSD) graph, which used to assessed the complex's dynamic stability during simulation [39], showed an increase in the first 30 ns, however, it remained stable for the rest of the trajectory and ended up with a RMSD value close to 0.3 Å (Fig. 5O). The root mean square fluctuation (RMSF) was used to study the time-dependent fluctuation of the complexes [39,40]. Results showed that the amino acid residues at positions 236, 257, 261–263, 419–421 and 468 had larger RMSF values, indicating that the flexibility of PPARα protein (Fig. 5P). The solvent-accessible surface aera (SASA) analysis showed a stable range of 140–150 nm^2 (Fig. 5Q). The radius of gyration (Rg) indicates the stability and density of the protein structure [41], and our results showed that the overall Rg value of the protein in the complex system remained between 1.9 and 2.0 (Fig. 5R), indicating that the structure of the proteins forming the complex remained dense throughout the simulation. As shown in Fig. 5S–W, the LYC was consistently located within the PPARα protein active site throughout the simulation. Moreover, amino acid residues that are crucial in LYC binding include Lys429, Phe365, Leu433 and others (Fig. 5X). Additionally, a total of 23 Alkyl and 3 Pi-Alkyl interactions were formed in the docking structure of LYC with PPARα. Collectively, all these results demonstrated that LYC could activate hepatic PPARα/FGF21 signalling, which was suppressed in the aging mice.

3.7. *FGF21 is required for the beneficial effects of LYC on brain function*

Circulating FGF21 originates from the liver under normal physiologic conditions [19,20], and hepatic FGF21 signal helps link the liver with CNS [16,18,24]. Mice were injected with AAV-shFGF21 through the tail vein to knock down FGF21 in aging mice. This was done to verify the importance of hepatic FGF21 signal in LYC improving age-related cognitive deficits. Subsequently, LYC was supplemented for 3 months (Fig. 6A). The *in vivo* silencing effects of AAV-shFGF21 treatment were evaluated first and results showed that AAV-shFGF21 treatment markedly reduced the FGF21 expression in mice liver and cortex (S. Fig. 3A–D) and this inhibition was maintained till the end of LYC intervention (Fig. 6B–F).

We also assessed the effects of AAV-shFGF21 treatment on mice learning and memory ability through the Y-maze test. Results showed that mice in the AAV-shFGF21 group showed decreased working memory capacity compared with those in the Aging + LYC group (Fig. 6G and H). FGF21 knockdown also accelerated brain senescence (Fig. 6I–K), leaded to neuronal degeneration and loss (Fig. 6L–Q),

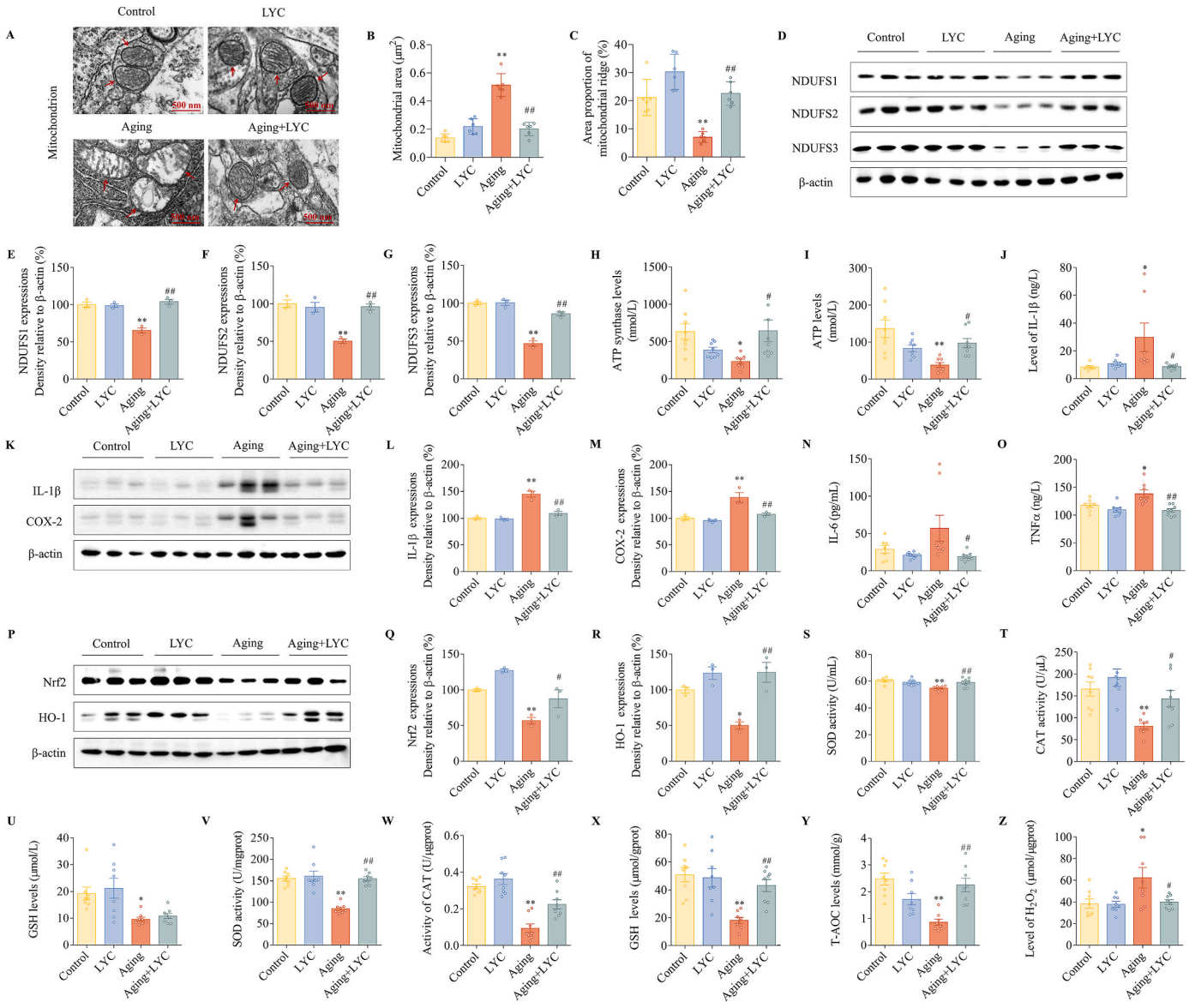

Fig. 4. Effects of LYC on aging-induced mitochondrial dysfunction, neuroinflammation and oxidative stress.
(A) Representative electron micrograph of mitochondria in hippocampus (the arrows indicated mitochondrion), n = 6. Quantitative analysis for (B) mitochondrial area, (C) area proportion of mitochondrial ridge. (D) Protein expressions of NDUFS1, NDUFS2 and NDUFS3 in the cortex of mice. Densitometry analyses were shown in (E)–(G). (H) ATP synthase levels in cortex. (I) ATP levels in cortex. (J) ELISA kits assay for IL-1β level in cortex. (K) Protein expressions of IL-1β and COX-2 in cortex. Densitometry analyses were shown in (L) & (M). ELISA kits assay for (N) IL-6 and (O) TNFα levels of in cortex. (P) Protein expressions of Nrf2 and HO-1 in cortex. Densitometry analyses were shown in (Q) & (R). Activities of (S) SOD, (T) CAT and (U) levels of GSH in plasma. Activities of (V) SOD, (W) CAT and levels of (X) GSH, (Y) T-AOC in cortex. (Z) Levels of H_2O_2 in cortex. $^{*}p < 0.05$, $^{**}p < 0.01$ versus Control group, $^{\#}p < 0.05$, $^{\#\#}p < 0.01$ versus Aging group.

decreased the plasticity of synaptic ultrastructure (Fig. 6R–T), and down-regulated PSD-95 (S. Fig. 3F–K) and BDNF (S. Fig. 3L–O) expression in the hippocampus and cortex of mice.

Moreover, AAV-shFGF21 treatment can be detrimental to synaptic vesicle fusion by suppressing the interaction between SNAP-25, VAMP and syntaxin in the cortex of mice (Fig. 6U–X). In addition, it induced mitochondrial dysfunctional in the hippocampus and cortex (Fig. 7A–F, S. Fig. 3E), down-regulated ATP synthase levels (Fig. 7G) and inhibited the production of ATP (Fig. 7H) in the cortex of mice when compared with the Aging + LYC group. Additionally, aggravated neuroinflammation in hippocampus and cortex (Fig. 7I–P, S. Fig. 3P–S), decreased antioxidant enzyme contents (Fig. 7Q–T), and increased MDA levels (S. Fig. 3T) in the cortex were also observed in FGF21 knockdown group mice. Overall, these results indicated that FGF21 is required for the protective effects of LYC on brain function in aging mice.

3.8. LYC improved hepatocytes supportive ability to neurons

Mouse hippocampal HT-22 cells were co-cultured with HepG2 in Transwell to further confirm the direct action of hepatocytes on neurons. HepG2 cells were treated with D-gal to establish aging cell mode [42, 43]. Exactly, 50 μM LYC and 10 mM D-gal were selected for subsequent experiments based on the cell viability test results (Fig. 8A–F). LYC administration to HepG2 significantly increased the FGF21 level in medium (Fig. 8G) and co-cultured neuronal cells (Fig. 8H), improved cell senescence in co-cultured neurons, characterized by decreased β-galactose content (Fig. 8I). This administration also improved mitochondrial morphology (Fig. 8K), decreased mitochondrial ROS and total cell ROS, elevated mitochondrial membrane potential (Fig. 8L–O-Q) and increased ATP levels (Fig. 8J) in co-cultured HT-22 cells. Moreover, axon lengths of co-cultured neurons were enhanced by LYC (Fig. 8M and

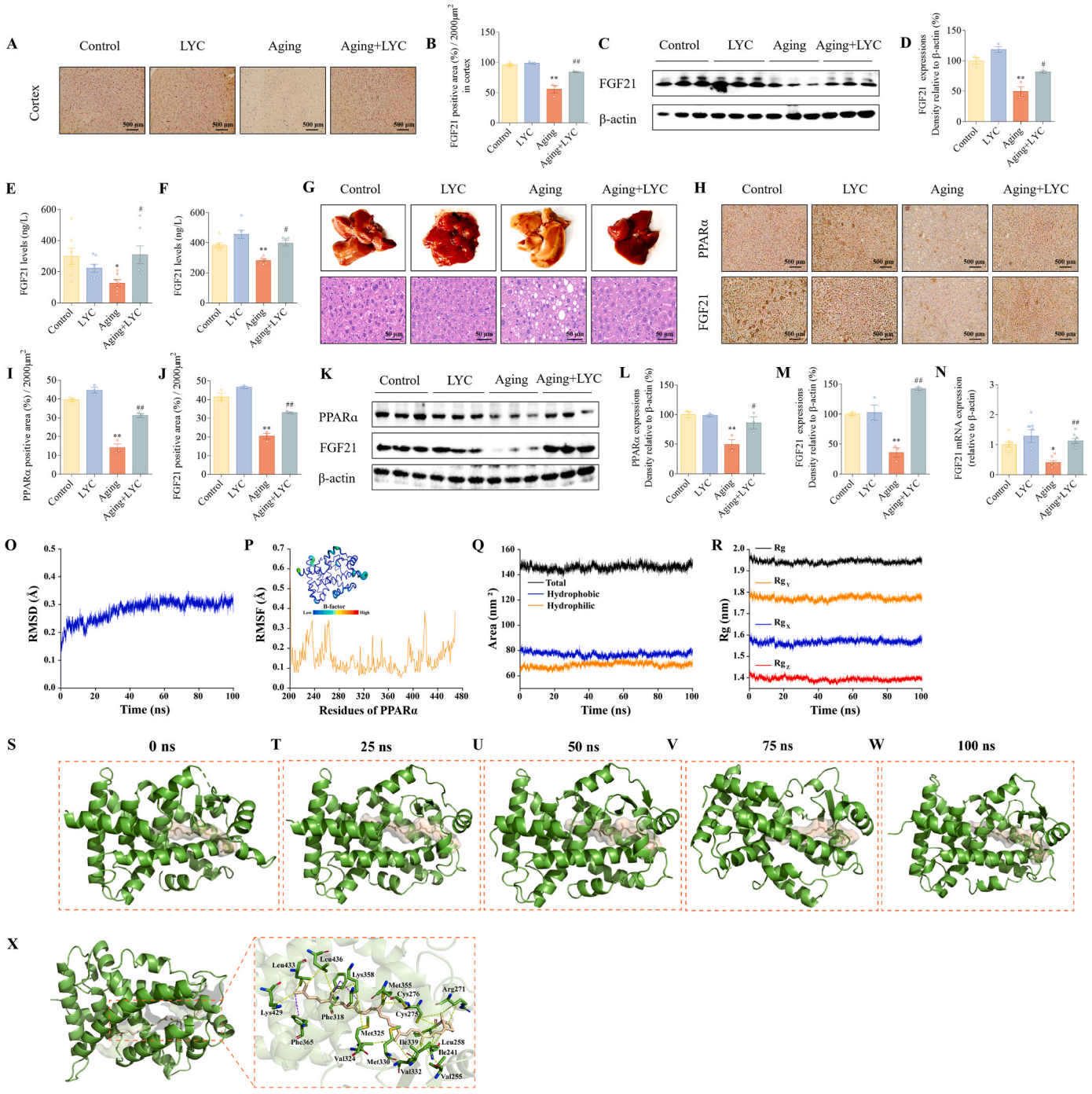

Fig. 5. Effects of LYC on FGF21 signal in liver-brain-axis.
(A) Immunohistochemical staining of FGF21 in the cortex of mice, n = 3. (B) Quantitative immunohistochemical analysis for evaluating FGF21 expression in cortex. (C) Protein expression of FGF21 in cortex. Densitometry analysis was shown in (D). ELISA kits assay for FGF21 levels in the (E) cortex and (F) plasma of mice. (G) Representative liver for each group and H&E staining of liver, n = 3. (H) Immunohistochemical staining of PPARα and FGF21 in liver, n = 3. Quantitative immunohistochemical analysis for evaluating (I) PPARα and (J) FGF21 expression in liver. (K) Protein expressions of PPARα and FGF21 in liver tissue. Densitometry analysis were shown in (L) & (M). (N) FGF21 mRNA expression in the cortex of mice. The graph of (O) RMSD, (P) RMSF, (Q) SASA and (R) Rg of PPARα-LYC complex. (S–W) The structure of docked complexes at 0, 25, 50, 75 and 100 ns during MD simulations. (X) Key residues surrounding LYC in the binding pocket of PPARα. $^{*}p < 0.05$, $^{**}p < 0.01$ versus Control group, $^{\#}p < 0.05$, $^{\#\#}p < 0.01$ versus Aging group.

N). All these findings indicated that LYC enhanced hepatocytes supportive ability to neurons.

3.9. FGF21 promoted synaptic vesicle fusion and neurotransmitters release

HT-22 cells were directly incubated with rFGF21 and results showed that FGF21 treatment enhanced mitochondrial function by improving mitochondrial morphology (Fig. 9A), decreasing mitochondrial ROS and intracellular total ROS (Fig. 9B–D), and restoring defective MMP (Fig. 9B and E). Moreover, FGF21 treatment elevated ATP synthetase level (Fig. 9F), increased ATP levels (Fig. 9G) in HT-22 cells and increased the levels of neurotransmitters in the medium (Fig. 9H–L), indicating that FGF21 treatment promoted neurotransmitter release in

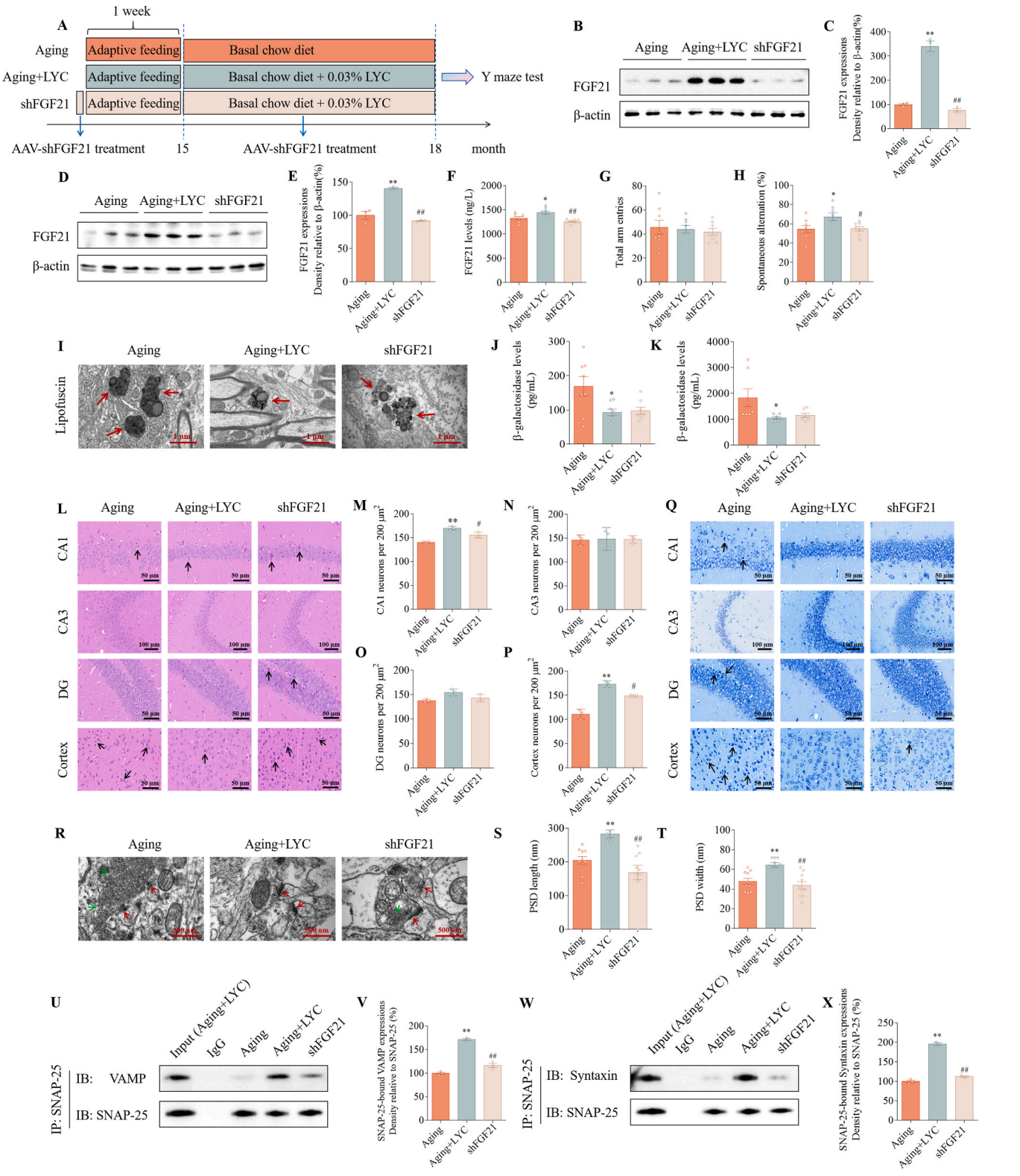

Fig. 6. FGF21 was required for LYC-mediated improvement of cognitive impairment in aging mice.
(A) Experimental scheme. Protein expression of FGF21 in mice (B) liver and (D) cortex. Densitometry analyses were shown in (C)&(E). (F) ELISA kits assay for FGF21 level in plasma. (G) Total arm entries and (H) spontaneous alternation in Y maze. (I) Lipofuscin in hippocampus (the arrows indicated lipofuscin), n = 6. β-galactosidase levels in (J) cortex and (K) plasma. (L) H&E staining in hippocampus and cortex (the arrows indicated shrunken and deformed neuronal cells), n = 3. (M)–(P) Neurons in hippocampus and cortex. (Q) Nissl staining in hippocampus and cortex (the arrows indicated shrunken and deformed neuronal cells), n = 3. (R) Representative electron micrograph of synaptosomal fractions from mice hippocampus (the red arrows indicated PSD and green arrows indicated synaptic vesicle), n = 6. The (S) length and (T) width of PSD. Co-IP and western blots analysis were used to evaluate the associativity of SNAP-25 and VAMP (U)&(V), SNAP-25 and syntaxin (W)&(X) in the cortex of mice. $^{*}p < 0.05$, $^{**}p < 0.01$ versus Aging group, $^{\#}p < 0.05$, $^{\#\#}p < 0.01$ versus Aging + LYC group.

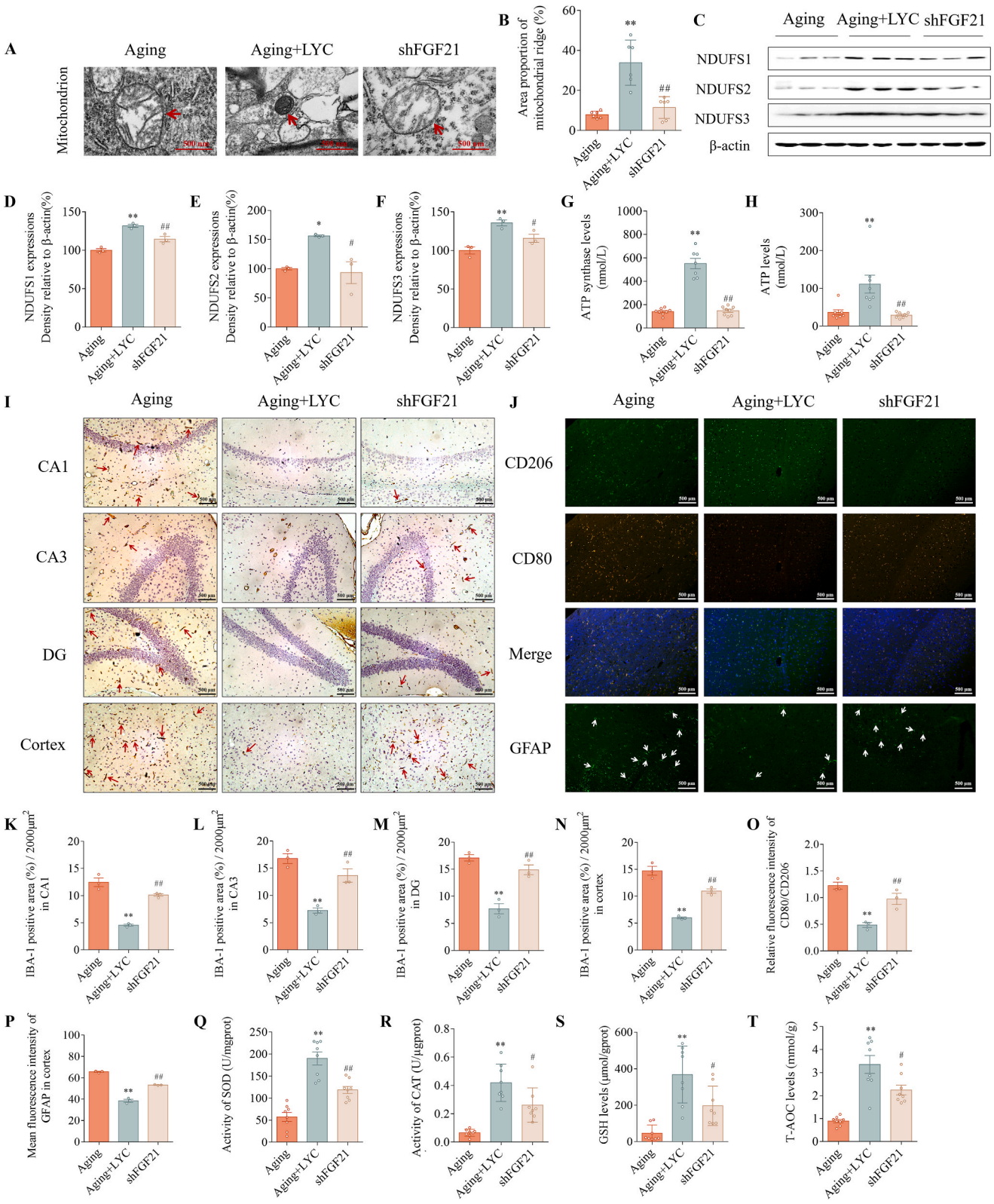

Fig. 7. FGF21 was required for LYC-mediated improvement of mitochondrial dysfunction, neuroinflammation and oxidative stress in aging mice.
(A) Representative electron micrograph of mitochondria in hippocampus (the arrows indicated mitochondrion), n = 6. (B) Quantitative analysis for area proportion of mitochondrial ridge. (C) Protein expressions of NDUFS1, NDUFS2 and NDUFS3 in the cortex of mice. Densitometry analyses were shown in (D)–(F). (G) ATP synthase levels in cortex. (H) ATP levels in cortex. (I) Immunohistochemical staining of IBA-1in hippocampus and cortex (the arrows indicated activated microglia), n = 3. (J) Immunofluorescence staining of CD206, CD80 and GFAP (the arrows indicated activated astrocytes) in the cortex, n = 3. Quantitative immunohistochemical analysis for evaluating activated microglia in (K) CA1, (L) CA3, (M) DG and (N) cortex regions. (O) Quantitative analysis for the relative fluorescence intensity of CD80/CD206. (P) Quantitative immunofluorescence analysis for evaluating activated astrocytes in cortex. Activities of (Q) SOD and (R) CAT in the cortex of mice. Levels of (S) GSH and (T) T-AOC in the cortex. $^{*}p < 0.05$, $^{**}p < 0.01$ versus Aging group, $^{\#}p < 0.05$, $^{\#\#}p < 0.01$ versus Aging + LYC group.

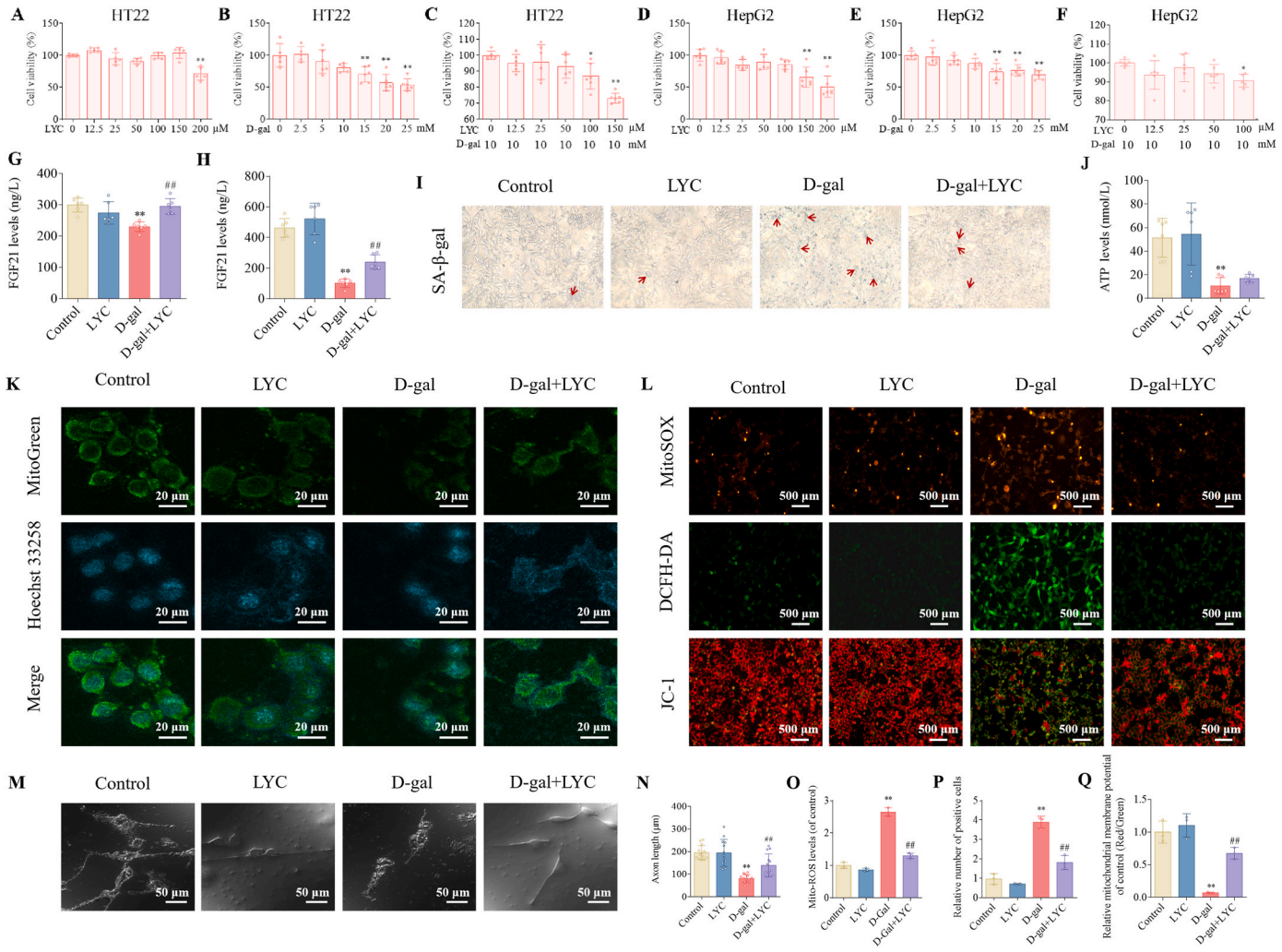

Fig. 8. LYC improved hepatocyte' supportive ability to neurons.
Effects of (A) LYC, (B) D-gal and (C) D-gal + LYC treatment on the cell viability of HT-22 cells. Effects of (D) LYC, (E) D-gal and (F) D-gal + LYC treatment on the cell viability of HepG2 cells. FGF21 level in (G) medium and (H) co-cultured HT-22 cells. (I) SA-β-gal staining in co-cultured HT-22 cells (the arrows indicated senescent cells), n = 3. (J) ATP levels in co-cultured HT-22 cells. (K) MitioGreen, (L) MitoSOX, DCFH-DA and JC-1 staining in co-cultured HT-22 cells, n = 3. (M) Images of co-cultured HT-22 cells, n = 3. (N) Analysis of axon length in co-cultured HT-22 cells. Quantitative analysis for evaluating (O) Mito-ROS levels, (P) intracellular ROS levels and (Q) mitochondrial membrane potential in co-cultured HT-22 cells. $^{*}p < 0.05$, $^{**}p < 0.01$ versus Control group, $^{\#}p < 0.05$, $^{\#\#}p < 0.01$ versus D-gal group.

HT-22 cells. Next, ATP synthesis inhibitor oligomycin was used to explore the mitochondrial effects on neurotransmitters release during this process. Results showed that when mitochondrial ATP synthesis was suppressed by oligomycin (Fig. 9M), the beneficial effects of FGF21 on neurotransmitters release were also blocked (Fig. 9N–R). Furthermore, we investigated the effects of FGF21 on the synaptic vesicle fusion process. Co-IP and western blots analysis revealed that FGF21 treatment enhanced the associativity of SNAP-25, VAMP and syntaxin in HT-22 cells (Fig. 9S–V). These results indicated that FGF21 in CNS promoted the production of ATP and enhanced the interaction between SNAREs core complex, all these changes promoted the release of neuronal neurotransmitters in the FGF21 group.

4. Discussion

Dietary LYC is absorbed by intestinal epithelial cells and stored in the liver, where it exerts its biological activity [12]. LYC has shown excellent neuroprotective properties in various animal models [8–10]. Our previous studies revealed that supplementing with LYC (0.03 %, w/w, mixed into normal chow diet) for 5 weeks alleviated cognitive deficits caused by systemic inflammation [44]. In addition, LYC (0.03 %, w/w) administration for 8 weeks improved D-gal-induced mitochondrial dysfunction [10]. Regarding this LYC's effect on cognitive deficits, we chose 0.03 % LYC supplementation (approximately 42.16 mg/kg/day) to analyze its neuroprotective effects on aging mice and explore the possible role of liver-brain FGF21 signal during these process in the present study.

Encephalopathy can result from acute hepatic failure or chronic hepatitis [14]. Reportedly, non-alcoholic steatohepatitis induces brain pathology, including neuroinflammation and neurodegeneration [15]. Kim et al. demonstrated that a high-fat diet (HFD)-induced chronic non-alcoholic fatty liver disease resulted in advanced pathological signs of Alzheimer's disease in wild-type mice. However, withdrawing the HFD decreased β-amyloid plaque load [45], suggesting that liver injury can influence CNS diseases. Hence maintaining liver health can possibly improve brain function. Liver FGF21 is an important signalling that links the liver and brain [16,18,24], and PPARα mediates hepatic FGF21 [24]. Additionally, PPARα can be modulated by multiple natural products, including tomato extracts [37,38]. Our results showed that LYC forms a stable complex with PPARα. There results showing FGF21 levels in the liver-brain axis during aging remain inconsistent. Ren et al. illustrated that FGF21 levels decreased with age in 15- and 18-month-old mice

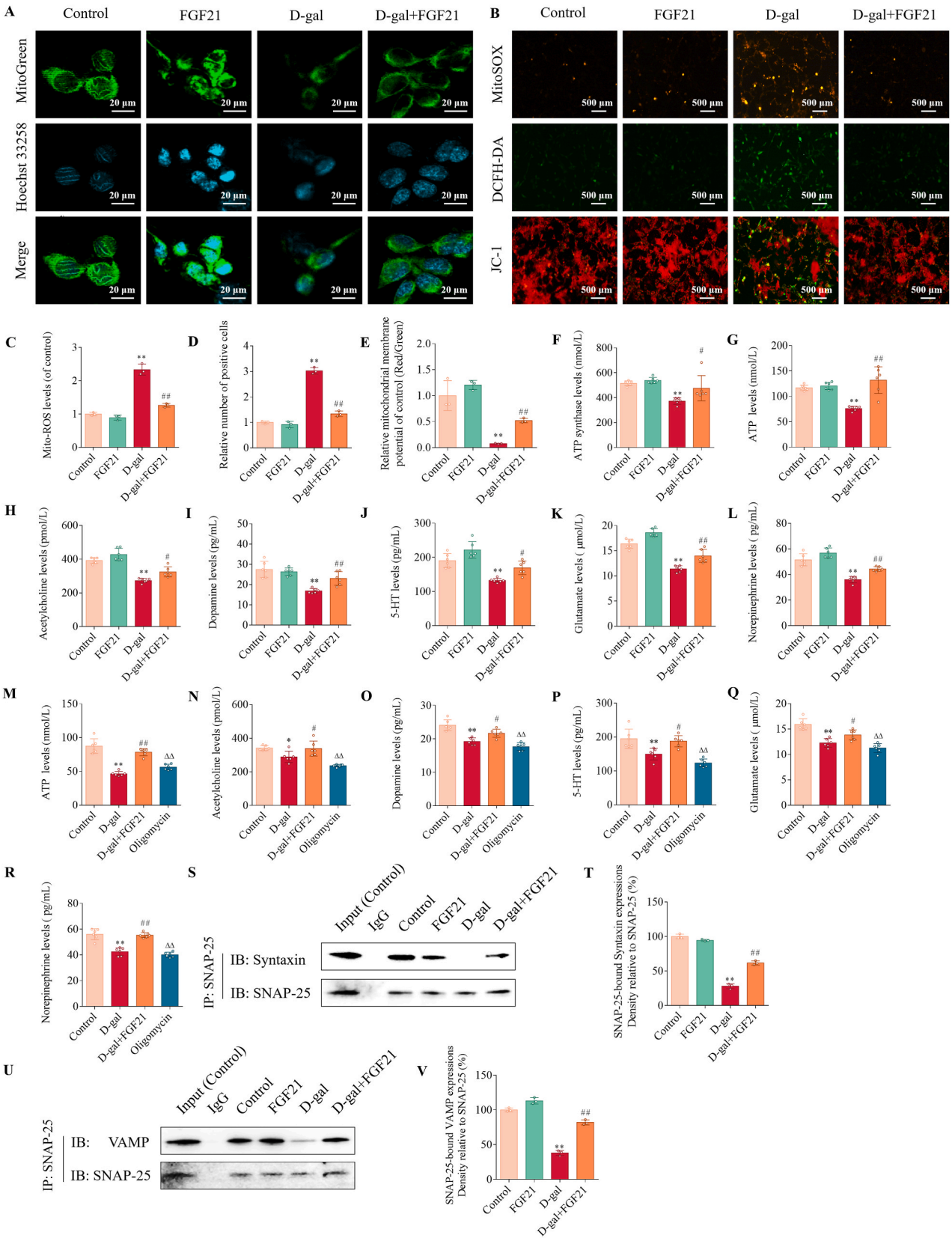

Fig. 9. Effects of FGF21 on mitochondrial function, synaptic vesicle fusion and neurotransmitters release.
(A) MitoGreen, (B) MitoSOX, DCFH-DA and JC-1 staining in HT-22 cells, n = 3. (C) Mito-ROS levels, (D) intracellular ROS levels and (E) mitochondrial membrane potential in HT-22 cells. (F) ATP synthase levels in HT-22 cells. (G) ATP levels in HT-22 cells. (H)–(L) Neurotransmitterins levels in medium. (M) ATP levels in HT-22 cells. (N)–(R) Neurotransmitterins levels in medium. Co-IP and western blots analysis were used to evaluate the associativity of SNAP-25 and syntaxin (S)&(T), SNAP-25 and VAMP (U)&(V) in HT-22 cells. *$p < 0.05$, **$p < 0.01$ versus Control group, $^{\#}p < 0.05$, $^{\#\#}p < 0.01$ versus D-gal group. $^{\triangle}p < 0.05$, $^{\triangle\triangle}p < 0.01$ versus D-gal + FGF21 group.

serum, liver, and brain [26]. In contrast, Matsui et al. reported that aging increases FGF21 levels in plasma [46]. In our study, lower levels of FGF21 in liver, brain and plasma in 18-month old mice were observed. However, LYC treatment increased the mRNA and protein expression of FGF21 in the liver, suggesting that it enhanced the transcriptional activity of PPARα. The underlying mechanism may involve LYC binding with PPARα to form a stable complex, potentially altering the molecular structure of PPARα and thereby affecting its transcriptional activity. Moreover, LYC also restored the FGF21 levels in mice brain and plasma. Additionally, we observed an interaction between PPARα and FGF21 (S. Fig. 2J and K). However, it remains unclear whether this interaction is linked to the enhanced transcriptional activity of PPARα or the neuroprotective effects of LYC. This warrants further investigation in future studies.

Furthermore, FGF21 is considered a pro-longevity hormone [47,48]. Because it alleviates senescence, apoptosis, and extracellular matrix degradation in osteoarthritis [47]. Additionally, it inhibits the accumulation of senescence markers SASP, P53, and P16 in the livers of aging mice [48]. In this study, FGF21 knockdown reversed LYC-improved brain aging, indicated by increased lipofuscin accumulation in the hippocampus of aging mice. Moreover, FGF21 has the ability to improve cognitive decline [26,49]. For example, recombinant FGF21 improved the learning and memory defects in diabetic mice [49]. However, knockdown of FGF21 impaired the cognitive function in methionine restriction-treated aging mice [26]. Similar results were obtained in our present study. Furthermore, LYC treatment for 3 months alleviated aging-induced hippocampal-dependent spatial learning impairment. However, these cognitive benefits were diminished when mice were injected with AAV-shFGF21 through the tail vein blocking the delivery of hepatic FGF21 to the brain.

Notably, brain function depends on communication between neurons through the precise regulation of synaptic vesicle fusion and neurotransmitter release [29]. In the present study, LYC partly mitigated aging-induced accumulation of synaptic vesicles at presynaptic sites. However, AAV-shFGF21 treatment aggravated the accumulation of synaptic vesicles. Hence, we analyzed the synaptic vesicle fusion processes to further reveal related molecular mechanisms. Notably, neuronal SNAREs core complex SNAP-25, VAMP, and syntaxin are critical for synaptic vesicle fusion and neurotransmitters release [30,31,50]. These SNAREs proteins interact to establish continuity between the opposing bilayers and catalyse membrane fusion when the active zone on the syntaxin and SNAP-25-associated plasma membrane is exposed to the VAMP-associated vesicle membrane [30]. Furthermore, substantial mitochondrial ATP consumption is required for synaptic vesicle recycling and neurotransmitter refilling [32]. Our results showed that LYC promoted the associativity of SNAREs core complex SNAP-25, VAMP and syntaxin *in vivo* and *in vitro*, suggesting an underlying mechanism for LYC to promote synaptic vesicle fusion. Notably, LYC also improved aging-induced mitochondrial dysfunction and promoted the production of ATP *in vivo* and *in vitro*. However, when mice received AAV-shFGF21, these benefits were inhibited, suggesting that FGF21 is required for the beneficial effects of LYC on synaptic vesicle fusion and neurotransmitter release. As expected, *in vitro* studies showed that when the HT-22 cells were incubated directly with FGF21, it promoted the release of neurotransmitters via enhancing the associativity of SNAREs core complex SNAP-25, VAMP and syntaxin, and increasing the production of ATP.

In addition to synaptic vesicle fusion and neurotransmitter release, LYC can exert its neuroprotective effect through various signalling pathways, and the hippocampus plays a critical role in memory and cognition [51]. In our study, LYC supplementation effectively reversed aging-induced neuronal degeneration and loss in the hippocampus and cortex. In addition, it improved the synaptic structural integrity. However, Ren et al. reported that FGF21 knockdown did not affect the morphology of neurons in the hippocampus [26]. The difference with his research is that AAV-shFGF21 treatment aggregated neuronal nuclei shrinkage and loss in the hippocampus and cortex when compared with the Aging + LYC group in our present study. Furthermore, AAV-shFGF21 damaged the synaptic structural integrity and decreased the expression of PSD-95, a key component of the postsynaptic membrane [52]. Neurotrophic factors are essential for normal neuronal activity and are crucial for synaptic function [28]. The positive effects of LYC on neurotrophic factors such as BDNF in aging mice were partly reversed by AAV-shFGF21. Additionally, AAV-shFGF21 treatment caused the over-activation of microglia and astrocytes and decreased antioxidant enzyme contents when compared with the Aging + LYC group. These results align with previous research showing that FGF21 alleviates chronic inflammatory injury in the aging process [48], reduces the expressions of pro-inflammatory factors: ionized calcium-binding adaptor molecule-1 (IBA-1), IL-6, and IL-8, and enhanced anti-oxidant enzymes in aging and diabetic mice [53]. All these might results from LYC's enhancement of cognitive function in aging mice through activating FGF21 signalling.

Lastly, we further explored the direct action of hepatocytes on neurons. HepG2 cells [54,55] and mouse hippocampal HT-22 cells [56,57] are often used in the food nutrition and health research. We performed HepG2-HT-22 co-culture experiments in Transwell, treating HepG2 cells with D-gal to establish an aging cell model [42,43]. The results showed that LYC intervention promoted the production and delivery of FGF21 in HepG2 cells to HT-22 cells. Furthermore, LYC enhanced the functional support of hepatocytes to neuronal cells. It alleviated D-gal-induced cellular senescence and mitochondrial dysfunction in co-cultured HT-22 cells. Considering that primary cells maintain more important functions, our future studies will focus on co-culture experiments with primary hepatocytes-primary neurons.

In conclusion, this study confirmed that FGF21, an endogenous hormonal signal from the liver to the brain, is required for LYC to regulate neuronal vesicle fusion, promote neurotransmitter release and thus improve cognitive ability in aging mice.

CRediT authorship contribution statement

Jia Wang: Writing – review & editing. **Lu Li:** Project administration. **Li Li:** Project administration. **Yuqi Shen:** Project administration. **Fubin Qiu:** Investigation.

Declaration of Competing interest

The authors declare that they have no conflict of interest.

Data availability

Data will be made available on request.

Acknowledgements

This work was supported by the National Natural Science Foundation of China (82103840), Applied Basic Research Program of Shanxi (20210302124642), Scientific and Technological Innovation Programs of Higher Education Institutions in Shanxi (2020L0175), Startup Foundation for Doctors of Shanxi Province (SD1914) and Startup Foundation for Doctors of Shanxi Medical University (XD1914).

Abbreviations

AAV	Adeno-associated virus
ATP	Adenosine triphosphate
BBB	Blood-brain barrier
CAT	Catalase
CNS	Central nervous system
CSF	Cerebrospinal fluid
Co-IP	Co-immunoprecipitation
D-gal	D-galactose

FMT	Fecal microbiota transplantation
FGF21	Fibroblast growth factor-21
GSH	Glutathione
H&E	Haematoxylin and eosin
HFD	High-fat diet
IL-1β	Interleukin 1beta
IL-6	Interleukin 6
IHC	Immunohistochemical
IBA-1	Ionized calcium-binding adaptor molecule-1
LYC	Lycopene
MDA	Malondialdehyde
MD	Molecular modeling
PSD	Postsynaptic density
Rg	Radius of gyration
ROS	Reactive oxygen species
rFGF21	Recombinant FGF21
SA-β-gal	Senescence associated-beta-galactosidase
SCFAs	|Short-chain fatty acids
SOD	Superoxide dismutase
TNFα	Tumor necrosis factor alpha

Appendix A. Supplementary data

Supplementary data to this article can be found online at https://doi.org/10.1016/j.redox.2024.103363.

References

[1] M. Moqri, C. Herzog, J.R. Poganik, Biomarkers of Aging Consortium, J. Justice, D. W. Belsky, A. Higgins-Chen, A. Moskalev, G. Fuellen, A.A. Cohen, I. Bautmans, M. Widschwendter, J. Ding, A. Fleming, J. Mannick, J.J. Han, A. Zhavoronkov, N. Barzilai, M. Kaeberlein, S. Cummings, B.K. Kennedy, L. Ferrucci, S. Horvath, E. Verdin, A.B. Maier, M.P. Snyder, V. Sebastiano, V.N. Gladyshev, Biomarkers of aging for the identification and evaluation of longevity interventions, Cell 186 (2023) 3758–3775, https://doi.org/10.1016/j.cell.2023.08.003.

[2] C. Reitz, M.A. Pericak-Vance, T. Foroud, R. Mayeux, A global view of the genetic basis of Alzheimer disease, Nat. Rev. Neurol. 19 (2023) 261–277, https://doi.org/10.1038/s41582-023-00789-z.

[3] C. Lopez-Lee, E.R.S. Torres, G. Carling, L. Gan, Mechanisms of sex differences in Alzheimer's disease, Neuron 112 (2024) 1208–1221, https://doi.org/10.1016/j.neuron.2024.01.024.

[4] E.J. Calabrese, M. Nascarella, P. Pressman, A.W. Hayes, G. Dhawan, R. Kapoor, V. Calabrese, E. Agathokleous, Hormesis determines lifespan, Ageing Res. Rev. 94 (2024) 102181, https://doi.org/10.1016/j.arr.2023.102181.

[5] R. Wei, Q. Lin, M. Adu, H. Huang, Z. Yan, F. Shao, G. Zhong, Z. Zhang, Z. Sang, L. Cao, Q. Ma, The sources, properties, extraction, biosynthesis, pharmacology, and application of lycopene, Food Funct. 14 (2023) 9974–9998, https://doi.org/10.1039/d3fo03327a.

[6] X. Gao, B. Lin, C. Chen, Z. Fang, J. Yang, S. Wu, Q. Chen, K. Zheng, Z. Yu, Y. Li, X. Gao, G. Lin, L. Chen, Lycopene from tomatoes and tomato products exerts renoprotective effects by ameliorating oxidative stress, apoptosis, pyroptosis, fibrosis, and inflammatory injury in calcium oxalate nephrolithiasis: the underlying mechanisms, Food Funct. 15 (2024) 4021–4036, https://doi.org/10.1039/d4fo00042k.

[7] R. Zhu, B. Chen, Y. Bai, T. Miao, L. Rui, H. Zhang, B. Xia, Y. Li, S. Gao, X. Wang, D. Zhang, Lycopene in protection against obesity and diabetes: a mechanistic review, Pharmacol. Res. 159 (2020) 104966, https://doi.org/10.1016/j.phrs.2020.104966.

[8] Q. Zhu, Z. Gao, J. Peng, C. Liu, X. Wang, S. Li, H. Zhang, Lycopene alleviates chronic stress-induced hippocampal microglial pyroptosis by inhibiting the cathepsin B/NLRP3 signaling pathway, J. Agric. Food Chem. 71 (2023) 20034–20046, https://doi.org/10.1021/acs.jafc.3c02749.

[9] H. Wang, M. Li, J. Cui, H. Zhang, Y. Zhao, J. Li, Lycopene prevents phthalate-induced cognitive impairment via modulating ferroptosis, J. Agric. Food Chem. 71 (2023) 16727–16738, https://doi.org/10.1021/acs.jafc.3c04801.

[10] J. Wang, Y. Shen, M. Li, T. Li, D. Shi, S. Lu, F. Qiu, Z. Wu, Lycopene attenuates D-galactose-induced cognitive decline by enhancing mitochondrial function and improving insulin signaling in the brains of female CD-1 mice, J. Nutr. Biochem. 118 (2023) 109361, https://doi.org/10.1016/j.jnutbio.2023.109361.

[11] J. Li, X. Zeng, X. Yang, H. Ding, Lycopene ameliorates skin aging by regulating the insulin resistance pathway and activating SIRT1, Food Funct. 13 (2022) 11307–11320, https://doi.org/10.1039/d2fo01111e.

[12] J. Wang, T. Li, M. Li, D. Shi, X. Tan, F. Qiu, Lycopene attenuates D-galactose-induced insulin signaling impairment by enhancing mitochondrial function and suppressing the oxidative stress/inflammatory response in mouse kidneys and livers, Food Funct. 13 (2022) 7720–7729, https://doi.org/10.1039/d2fo00706a.

[13] T. Liu, J. Li, Q. Li, Y. Liang, J. Gao, Z. Meng, P. Li, M. Yao, J. Gu, H. Tu, Y. Gan, Environmental eustress promotes liver regeneration through the sympathetic regulation of type 1 innate lymphoid cells to increase IL-22 in mice, Hepatology 78 (2023) 136–149, https://doi.org/10.1097/HEP.0000000000000239.

[14] R. Bordet, D. Deplanque, Brain-liver axis: a new pathway for cognitive disorders related to hepatic fibrosis, Eur. J. Neurol. 27 (2020) 2111–2112, https://doi.org/10.1111/ene.14454.

[15] A. Mondal, D. Bose, P. Saha, S. Sarkar, R. Seth, D. Kimono, M. Albadrani, M. Nagarkatti, P. Nagarkatti, S. Chatterjee, Lipocalin 2 induces neuroinflammation and blood-brain barrier dysfunction through liver-brain axis in murine model of nonalcoholic steatohepatitis, J. Neuroinflammation 17 (2020) 201–215, https://doi.org/10.1186/s12974-020-01876-4.

[16] F.M. Fisher, E. Maratos-Flier, Understanding the physiology of FGF21, Annu. Rev. Physiol. 78 (2016) 223–241, https://doi.org/10.1146/annurev-physiol-021115-105339.

[17] E. Szczepańska, M. Gietka-Czernel, FGF21: a novel regulator of glucose and lipid metabolism and whole-body energy balance, Horm. Metab. Res. 54 (2022) 203–211, https://doi.org/10.1055/a-1778-4159.

[18] Q. Liang, L. Zhong, J. Zhang, Y. Wang, S.R. Bornstein, C.R. Triggle, H. Ding, K.S. L. Lam, A. Xu, FGF21 maintains glucose homeostasis by mediating the cross talk between liver and brain during prolonged fasting, Diabetes 63 (2014) 4064–4075, https://doi.org/10.2337/db14-0541.

[19] O. Stöhr, R. Tao, J. Miao, K.D. Copps, M.F. White, FoxO1 suppresses Fgf21 during hepatic insulin resistance to impair peripheral glucose utilization and acute cold tolerance, Cell Rep. 34 (2021) 108893, https://doi.org/10.1016/j.celrep.2021.108893.

[20] K.R. Markan, M.C. Naber, M.K. Ameka, M.D. Anderegg, D.J. Mangelsdorf, S. A. Kliewer, M. Mohammadi, M.J. Potthoff, Circulating FGF21 is liver derived and enhances glucose uptake during refeeding and overfeeding, Diabetes 63 (2014) 4057–4063, https://doi.org/10.2337/db14-0595.

[21] S. Chen, S. Chen, Y. Sun, Z. Xu, Y. Wang, S. Yao, W. Yao, X. Gao, Fibroblast growth factor 21 ameliorates neurodegeneration in rat and cellular models of Alzheimer's disease, Redox Biol. 22 (2019) 101133, https://doi.org/10.1016/j.redox.2019.101133.

[22] M. Choi, M. Schneeberger, W. Fan, A. Bugde, L. Gautron, K. Vale, R.E. Hammer, Y. Zhang, J.M. Friedman, D.J. Mangelsdorf, S.A. Kliewer, FGF21 counteracts alcohol intoxication by activating the noradrenergic nervous system, Cell Metab. 35 (2023) 429–437, https://doi.org/10.1016/j.cmet.2023.02.005.

[23] B.K. Tan, M. Hallschmid, R. Adya, W. Kern, H. Lehnert, H.S. Randeva, Fibroblast growth factor 21 (FGF21) in human cerebrospinal fluid: relationship with plasma FGF21 and body adiposity, Diabetes 60 (2011) 2758–2762, https://doi.org/10.2337/db11-0672.

[24] L. Geng, K.S.L. Lam, A. Xu, The therapeutic potential of FGF21 in metabolic diseases: from bench to clinic, Nat. Rev. Endocrinol. 16 (2020) 654–667, https://doi.org/10.1038/s41574-020-0386-0.

[25] S. Minami, S. Sakai, T. Yamamoto, Y. Takabatake, T. Namba-Hamano, A. Takahashi, J. Matsuda, H. Yonishi, J. Nakamura, S. Maeda, S. Matsui, I. Matsui, Y. Isaka, FGF21 and autophagy coordinately counteract kidney disease progression during aging and obesity, Autophagy 20 (2024) 489–504, https://doi.org/10.1080/15548627.2023.2259282.

[26] B. Ren, L. Wang, L. Shi, X. Jin, Y. Liu, R.H. Liu, F. Yin, E. Cadenas, X. Dai, Z. Liu, X. Liu, Methionine restriction alleviates age-associated cognitive decline via fibroblast growth factor 21, Redox Biol. 41 (2021) 101940, https://doi.org/10.1016/j.redox.2021.101940.

[27] C. López-Otín, M.A. Blasco, L. Partridge, M. Serrano, G. Kroemer, Hallmarks of aging: an expanding universe, Cell 186 (2023) 243–278, https://doi.org/10.1016/j.cell.2022.11.001.

[28] P.C. Casarotto, M. Girych, S.M. Fred, V. Kovaleva, R. Moliner, G. Enkavi, C. Biojone, C. Cannarozzo, M.P. Sahu, K. Kaurinkoski, C.A. Brunello, A. Steinzeig, F. Winkel, S. Patil, S. Vestring, T. Serchov, C.R.A.F. Diniz, L. Laukkanen, I. Cardon, H. Antila, T. Rog, T.P. Piepponen, C.R. Bramham, C. Normann, S.E. Lauri, M. Saarma, I. Vattulainen, E. Castrén, Antidepressant drugs act by directly binding to TRKB neurotrophin receptors, Cell 184 (2021) 1299–1313, https://doi.org/10.1016/j.cell.2021.01.034.

[29] M.E. Soden, J.X. Yee, L.S. Zweifel, Circuit coordination of opposing neuropeptide and neurotransmitter signals, Nature 619 (2023) 332–337, https://doi.org/10.1038/s41586-023-06246-7.

[30] X. Wang, D. Yu, H. Wang, Z. Lei, Y. Zhai, M. Sun, S. Chen, P. Yin, Rab3 and synaptotagmin proteins in the regulation of vesicle fusion and neurotransmitter release, Life Sci. 309 (2022) 120995, https://doi.org/10.3389/fnmol.2021.733138.

[31] K.P. Stepien, J. Rizo, Synaptotagmin-1-, Munc18-1-, and Munc13-1-dependent liposome fusion with a few neuronal SNAREs, Proc. Natl. Acad. Sci. U S A 118 (2021) e2019314118, https://doi.org/10.1073/pnas.2019314118.

[32] S. Li, Z. Sheng, Energy matters: presynaptic metabolism and the maintenance of synaptic transmission, Nat. Rev. Neurosci. 23 (2022) 4–22, https://doi.org/10.1038/s41583-021-00535-8.

[33] T. König, H.M. McBride, Mitochondrial-derived vesicles in metabolism, disease, and aging, Cell Metab. 36 (2024) 21–35, https://doi.org/10.1016/j.cmet.2023.11.014.

[34] J. Choi, S. Jo, D. Kim, I. Paik, R. Balakrishnan, Aerobic exercise attenuates LPS-induced cognitive dysfunction by reducing oxidative stress, glial activation, and neuroinflammation, Redox Biol. 71 (2024) 103101, https://doi.org/10.1016/j.redox.2024.103101.

[35] H.S. Kwon, S. Koh, Neuroinflammation in neurodegenerative disorders: the roles of microglia and astrocytes, Transl. Neurodegener. 9 (2020) 42–53, https://doi.org/10.1186/s40035-020-00221-2.
[36] Y. Sun, H. Zhu, R. Zhao, S. Zhou, M. Wang, Y. Yang, Z. Guo, Remote ischemic conditioning attenuates oxidative stress and inflammation via the Nrf2/HO-1 pathway in MCAO mice, Redox Biol. 66 (2023) 102852, https://doi.org/10.1016/j.redox.2023.102852.
[37] D. Rigano, C. Sirignano, O. Taglialatela-Scafati, The potential of natural products for targeting PPARα, Acta Pharm. Sin. B 7 (2017) 427–438, https://doi.org/10.1016/j.apsb.2017.05.005.
[38] Y. Kim, S. Hirai, H. Takahashi, T. Goto, C. Ohyane, T. Tsugane, C. Konishi, T. Fujii, S. Inai, Y. Iijima, K. Aoki, D. Shibata, N. Takahashi, T. Kawada, 9-oxo-10(E),12(E)-octadecadienoic acid derived from tomato is a potent PPAR α agonist to decrease triglyceride accumulation in mouse primary hepatocytes, Mol. Nutr. Food Res. 55 (2011) 585–593, https://doi.org/10.1002/mnfr.201000264.
[39] Y. Liao, P. Cao, L. Luo, Development of novel ALOX15 inhibitors combining dual machine learning filtering and fragment substitution optimisation approaches, molecular docking and dynamic simulation methods, J. Enzyme Inhib. Med. Chem. 39 (2024) 2301756, https://doi.org/10.1080/14756366.2024.2301756.
[40] U.A. More, M.N. Noolvi, D. Kumar, A. Tripathi, Exploring the molecular structural requirements of flavonoids as beta-secretase-1 inhibitors using molecular modeling studies, Curr. Drug Discov. Technol. 20 (2023) e290323215095, https://doi.org/10.2174/1570163820666230329090424.
[41] M. Iu Lobanov, N.S. Bogatyreva, O.V. Galzitskaia, Radius of gyration is indicator of compactness of protein structure, Mol. Biol. (Mosk). 42 (2008) 701–706.
[42] M. Ru, W. Wang, Z. Zhai, R. Wang, Y. Li, J. Liang, D. Kothari, K. Niu, X. Wu, Nicotinamide mononucleotide supplementation protects the intestinal function in aging mice and D-galactose induced senescent cells, Food Funct. 13 (2022) 7507–7519, https://doi.org/10.1039/d2fo00525e.
[43] H. Wang, Y. Sun, T. Qu, X. Sang, L. Zhou, Y. Li, F. Ren, Nobiletin prevents D-galactose-induced C2C12 cell aging by improving mitochondrial function, Int. J. Mol. Sci. 23 (2022) 11963, https://doi.org/10.3390/ijms231911963.
[44] J. Wang, L. Li, Z. Wang, Y. Cui, X. Tan, T. Yuan, Q. Liu, Z. Liu, X. Liu, Supplementation of lycopene attenuates lipopolysaccharide-induced amyloidogenesis and cognitive impairments via mediating neuroinflammation and oxidative stress, J. Nutr. Biochem. 56 (2018) 16–25, https://doi.org/10.1016/j.jnutbio.2018.01.009.
[45] D. Kim, A. Krenz, L.E. Toussaint, K.J. Maurer, S. Robinson, A. Yan, L. Torres, M. S. Bynoe, Non-alcoholic fatty liver disease induces signs of Alzheimer's disease (AD) in wild-type mice and accelerates pathological signs of AD in an AD model, J. Neuroinflammation 13 (2016) 1–18, https://doi.org/10.1186/s12974-015-0467-5.
[46] M. Matsui, K. Kosaki, K. Tanahashi, N. Akazawa, Y. Osuka, K. Tanaka, M. Kuro-O, S. Maeda, Relationship between physical activity and circulating fibroblast growth factor 21 in middle-aged and older adults, Exp. Gerontol. 141 (2020) 111081, https://doi.org/10.1016/j.exger.2020.111081.
[47] H. Lu, C. Jia, D. Wu, H. Jin, Z. Lin, J. Pan, X. Li, W. Wang, Fibroblast growth factor 21 (FGF21) alleviates senescence, apoptosis, and extracellular matrix degradation in osteoarthritis via the SIRT1-mTOR signaling pathway, Cell Death Dis. 12 (2021) 865–877, https://doi.org/10.1038/s41419-021-04157-x.
[48] K. Kang, A. Xia, F. Meng, J. Chunyu, X. Sun, G. Ren, D. Yu, X. Jiang, L. Tang, W. Xiao, D. Li, FGF21 alleviates chronic inflammatory injury in the aging process through modulating polarization of macrophages, Int. Immunopharmacol. 96 (2021) 107634, https://doi.org/10.1016/j.intimp.2021.107634.
[49] L. Zhao, H. Jiang, J. Xie, D. Shen, Q. Yi, J. Yan, C. Li, H. Zheng, H. Gao, Effects of fibroblast growth factor 21 on lactate uptake and usage in mice with diabetes-associated cognitive decline, Mol. Neurobiol. 59 (2022) 5656–5672, https://doi.org/10.1007/s12035-022-02926-z.
[50] F.J. López-Murcia, K. Reim, H. Taschenberger, Complexins: ubiquitously expressed presynaptic regulators of SNARE-mediated synaptic vesicle fusion, Adv. Neurobiol 33 (2023) 255–285, https://doi.org/10.1007/978-3-031-34229-5_10.
[51] Y. Vanrobaeys, U. Mukherjee, L. Langmack, S.E. Beyer, E. Bahl, L. Lin, J. J. Michaelson, T. Abel, S. Chatterjee, Mapping the spatial transcriptomic signature of the hippocampus during memory consolidation, Nat. Commun. 14 (2023) 6100–6114, https://doi.org/10.1038/s41467-023-41715-7.
[52] S. Xue, J. He, L. Lu, S. Song, M. Chen, F. Wang, J. Chen, Enhanced TARP-γ 8-PSD-95 coupling in excitatory neurons contributes to the rapid antidepressant-like action of ketamine in male mice, Nat. Commun. 14 (2023) 7971–7986, https://doi.org/10.1038/s41467-023-42780-8.
[53] K. Kang, P. Xu, M. Wang, J. Chunyu, X. Sun, G. Ren, W. Xiao, D. Li, FGF21 attenuates neurodegeneration through modulating neuroinflammation and oxidant-stress, Biomed. Pharmacother. 129 (2020) 110439, https://doi.org/10.1016/j.biopha.2020.110439.
[54] Z. Meng, B. Zhu, M. Gao, G. Wang, H. Zhou, J. Lu, S. Guan, Apigenin alleviated PA-induced pyroptosis by activating autophagy in hepatocytes, Food Funct. 13 (2022) 5559–5570, https://doi.org/10.1039/d1fo03771d.
[55] D. Shan, J. Wang, Q. Di, Q. Jiang, Q. Xu, Steatosis induced by nonylphenol in HepG2 cells and the intervention effect of curcumin, Food Funct. 13 (2022) 327–343, https://doi.org/10.1039/d1fo02481g.
[56] H. Hua, H. Zhu, C. Liu, W. Zhang, J. Li, B. Hu, Y. Guo, Y. Cheng, F. Pi, Y. Xie, W. Yao, H. Qian, Bioactive compound from the Tibetan turnip (Brassica rapa L.) elicited anti-hypoxia effects in OGD/R-injured HT-22 cells by activating the PI3K/AKT pathway, Food Funct. 12 (2021) 2901–2913, https://doi.org/10.1039/d0fo03190a.
[57] Y. Jiang, Y. Qi, X. Liu, L. Fang, Y. Gao, C. Liu, D. Wu, X. Wang, F. Zhao, J. Wang, W. Min, Neuroprotective effects of fermented yak milk-derived peptide LYLKPR on H_2O_2-injured HT-22 cells, Food Funct. 13 (2022) 12021–12038, https://doi.org/10.1039/d2fo02131e.